The origin of the anomalous superconducting properties of MgB_2

Hyoung Joon Choi*, David Roundy*†, Hong Sun*, Marvin L. Cohen*† & Steven G. Louie*†

* *Department of Physics, University of California at Berkeley, Berkeley, California 94720, USA*
† *Materials Sciences Division, Lawrence Berkeley National Laboratory, Berkeley, California 94720, USA*

Magnesium diboride[1] differs from ordinary metallic superconductors in several important ways, including the failure of conventional models[2] to predict accurately its unusually high transition temperature, the effects of isotope substitution on the critical transition temperature, and its anomalous specific heat[3–5]. A detailed examination of the energy associated with the formation of charge-carrying pairs, referred to as the 'superconducting energy gap', should clarify why MgB_2 is different. Some early experimental studies have indicated that MgB_2 has multiple gaps[3–9], but past theoretical studies[10–16] have not explained from first principles the origin of these gaps and their effects. Here we report an *ab initio* calculation of the superconducting gaps in MgB_2 and their effects on measurable quantities. An important feature is that the electronic states dominated by orbitals in the boron plane couple strongly to specific phonon modes, making pair formation favourable. This explains the high transition temperature, the anomalous structure in the specific heat, and the existence of multiple gaps in this material. Our analysis suggests comparable or higher transition temperatures may result in layered materials based on B, C and N with partially filled planar orbitals.

MgB_2 is a metal with a layer structure (Fig. 1a). The boron atoms form honeycombed layers, and the magnesium atoms are located above the centre of the hexagons in-between the boron planes. The electronic states at the Fermi level, which are the highest occupied electronic states, are mainly either σ- or π-bonding boron orbitals (Fig. 1b–d). The σ-bonding states are confined in the boron planes. Thus, MgB_2 may be unique with partially occupied σ-bonding states in a layer structure. Because the charge distribution of the σ-bonding states is not symmetrical with respect to the in-plane positions of boron atoms, the σ-bonding states couple very strongly to the in-plane vibration of boron atoms (Fig. 1e). We show that this strong coupling results in strong electron-pair formation of the σ-bonding states with an average energy gap Δ of 6.8 meV. This strong pairing, which is confined to the boron planes and to only parts of the Fermi surface, is the principal contribution responsible for the superconductivity. However, the π-bonding states on the remaining parts of the Fermi surface form much weaker pairs with an average Δ of 1.8 meV. This pairing is enhanced by the coupling to the σ-bonding states.

Our present theoretical work is based on the strong coupling formalism of superconductivity established by Eliashberg[17–19]. The Eliashberg formalism[17] is a more general extension of the original formulation of the Bardeen–Cooper–Schrieffer (BCS) theory, which is based on the mechanism for pairing that involves an attractive interaction between electrons mediated by lattice vibrations. This approach is able to reproduce successfully the superconducting transition temperature of MgB_2 after detailed material properties are used[16]. This particular study[16] provides only the transition temperature T_c, and does not give information on the superconducting energy gap (which is zero at T_c) or the temperature dependence of any measured quantities. However, the same general approach formally provides us with the nonlinear equations[18,19] for the superconducting energy gap at temperatures below the transition temperature. We solved this set of equations using an iterative technique[20] to obtain the full crystal momentum **k** and temperature dependence of the energy gap of MgB_2 from first principles. A two-gap structure is assumed in model calculations[14], and the ratio of the gap sizes obtained is consistent with the results presented here.

We have evaluated the properties of the superconducting energy gap of MgB_2 on the Fermi surface at low temperature (Fig. 2a, b). In MgB_2, the Fermi surface consists of two sheets from the σ-bonding states of boron $p_{x,y}$ orbitals, and two sheets from the π-bonding states of boron p_z orbitals. The calculation of the energy gap is made without any assumption of its functional shape on the Fermi surface. The resulting superconducting energy gap has *s*-wave

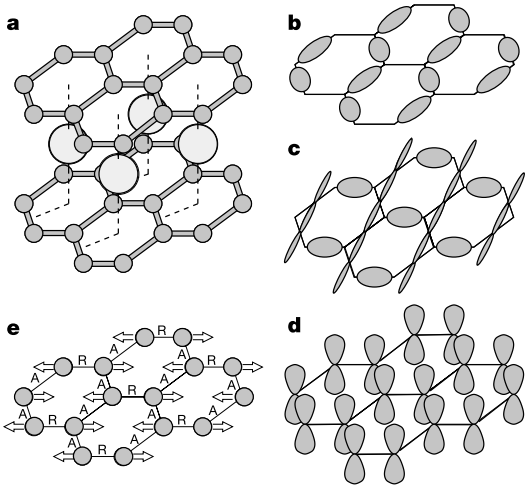

Figure 1 Crystal structure of MgB_2, electronic states at the Fermi level, and a vibrational mode of boron atoms. **a**, Crystal structure of MgB_2. Boron atoms form honeycomb planes, and magnesium atoms occupy the centres of the hexagons in-between boron planes. **b**, **c**, σ-bonding states at the Fermi level derived from boron $p_{x,y}$ orbitals. **d**, A π-bonding state at the Fermi level derived from boron p_z orbitals. **e**, A vibrational mode of boron atoms that couples strongly to σ-bonding electronic states at the Fermi level. As boron atoms move in the arrow directions, shortened bonds, marked with 'A', become attractive to electrons, whereas elongated bonds, marked with 'R', become repulsive. The σ-bonding states (**b**, **c**) couple strongly to the vibrational mode because they are mainly located in either the attractive or the repulsive bondings of the mode. The π-bonding states (**d**) do not couple strongly to this mode.

symmetry (that is, the gap is of the same sign and non-zero everywhere on the Fermi surface), but the size of the gap changes greatly on the different sections of the Fermi surface. The magnitude of the energy gap at 4 K ranges from 6.4 to 7.2 meV on the σ sheets, and from 1.2 to 3.7 meV on the π sheets (Fig. 2a, b). The average values of the gap are 6.8 meV for the σ sheets and 1.8 meV for the π sheets. In experimental measurements, there has been a debate on the number of gaps[3–9,21–26]. Our result is consistent with the recent experiments reporting two gaps, ranging from 1.5 to 3.5 meV for the small gap and 5.5 to 8 meV for the large gap[3–9,26].

The variation of the superconducting energy gap on the Fermi surface can be measured by techniques such as high-resolution angle-resolved photoelectron spectroscopy. Moreover, as the σ-bonding states are confined to the boron planes, the strong pairing gap of around 6.8 meV is associated with these planes (Fig. 2c). In Fig. 2c, we introduce the concept of a local gap distribution $\rho(\mathbf{r},\Delta)$ at position $\mathbf{r}$ given by $\rho(\mathbf{r},\Delta)=\sum_{\mathbf{k}}|\psi_{\mathbf{k}}(\mathbf{r})|^2\delta(\Delta-\Delta_{\mathbf{k}})$, where $\psi_{\mathbf{k}}(\mathbf{r})$ is the electron wavefunction with crystal momentum $\mathbf{k}$. Our result shows that the small gaps should be seen preferentially in tunnelling experiments along the c axis, as indicated in some recent measurements[6,7].

Figure 3a depicts the calculated superconducting energy gaps at various temperatures below the transition temperature. The energy gap of the σ-bonding states and that of the π-bonding states show different temperature dependences. Compared to the small energy gap of the π-bonding states, the large energy gap of the σ-bonding states changes more slowly at low temperature, but more rapidly near the transition temperature. Both the π and σ gaps vanish at the same transition temperature, although their values are greatly different at low temperatures[27]. This temperature dependence of the superconducting energy gaps explains recent tunnelling, optical and specific-heat measurements[3–9].

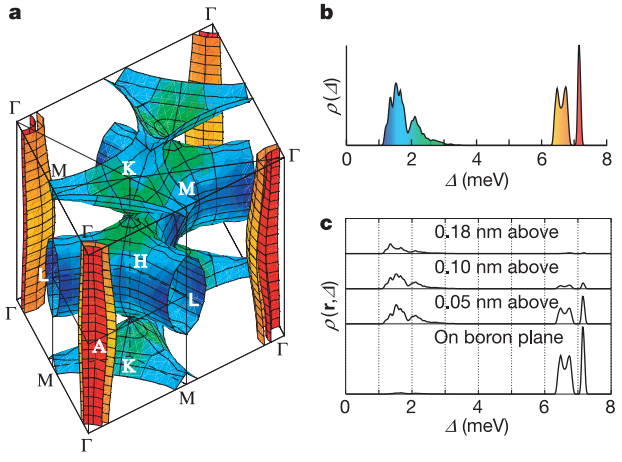

Figure 2 The superconducting energy gap of MgB_2. **a**, **b**, The superconducting energy gap on the Fermi surface at 4 K given using a colour scale (**a**), and the distribution of gap values at 4 K (**b**). The Fermi surface of MgB_2 consists of four distinctive sheets. Two σ sheets ('cylinders'), derived from the σ-bonding $p_{x,y}$ orbitals of boron, are shown split into eight pieces around the four vertical Γ–Γ lines. Two π sheets ('webbed tunnels'), derived from the π-bonding p_z orbitals of boron, are shown around K–M and H–L lines (upper and lower K–M lines are equivalent). The superconducting energy gap is ~7.2 meV on the narrower σ cylindrical sheet, shown in red, with variations of less than 0.1 meV. On the wider σ cylindrical sheet, shown in orange, the energy gap ranges from 6.4 to 6.8 meV, having a maximum near Γ and a minimum near A. On the π sheets, shown in green and blue, the energy gap ranges from 1.2 to 3.7 meV. The density of states at the Fermi energy is 0.12 states per (eV atom spin), 44% of which comes from the σ sheets and the other 56% comes from the π sheets. **c**, Local distribution of the superconducting energy gap on a boron plane and on planes at 0.05, 0.10 and 0.18 nm above a boron plane, respectively.

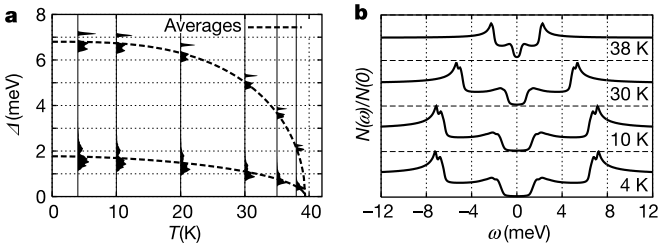

Figure 3 Calculated temperature dependence of the superconducting gaps and the quasiparticle density of states. **a**, Temperature dependence of the superconducting gaps. Vertical solid curves represent the distribution of the superconducting gap values at various temperatures from 4 K to 38 K. Dashed curves are of the form $\Delta(T)=\Delta(0)\times(1-(T/T_c)^p)^{1/2}$ fitted separately to the calculated average energy gap of the σ-bonding states and that of the π-bonding states. For the σ sheets, $\Delta(0)=6.8$ meV ($2\Delta(0)/k_BT_c=4.0$) (k_B = Boltzmann's constant) and $p=2.9$. For the π sheets, $\Delta(0)=1.8$ meV ($2\Delta(0)/k_BT_c=1.06$) and $p=1.8$. **b**, The quasiparticle density of states at various temperatures. The quasiparticle density of states $N(\omega)$ for the quasiparticle energy ω is given by $N(\omega)/N(0)=\mathrm{Re}\langle(\omega+i\Gamma)/((\omega+i\Gamma)^2-\Delta(\mathbf{k},\omega)^2)^{1/2}\rangle$, where $N(0)$ is the electron density of states at the Fermi level, $i=(-1)^{1/2}$, and $\langle\cdots\rangle$ indicates an average over a surface of constant ω. This curve is obtained from the calculated gap function $\Delta(\mathbf{k},\omega)$ and an assumed finite lifetime Γ of 0.1 meV.

The superconducting energy gap determines the quasiparticle density of states. The quasiparticle energy is the excitation energy of a system when an electron is added or removed. In a superconductor, the quasiparticle energy is equal to, or greater than, the superconducting energy gap Δ. Because the energy gap differs considerably for the σ- and π-bonding states in MgB_2, the density of quasiparticle excitations as a function of energy shows two thresholds (Fig. 3b). Only π-bonding quasiparticle states are allowed for energies between the minimal superconducting energy gap of the π-bonding states and that of the σ-bonding states. For energies above the minimal superconducting energy gap of the σ-bonding states, quasiparticle excitation becomes possible for both the σ- and π-bonding states. The quasiparticle density of states can be deduced experimentally from tunnelling experiments and var-

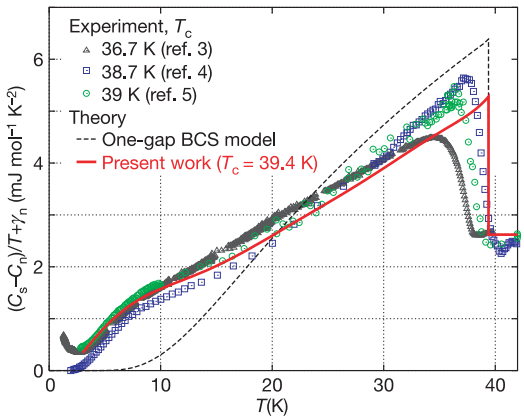

Figure 4 The specific heat of MgB_2. The measured and calculated electronic contribution to the specific heat divided by temperature are plotted as a function of temperature. The red solid curve represents the result of our calculation. The specific heat difference (C_S-C_N) between the superconducting and normal states is obtained by $C_S-C_N=-T(\mathrm{d}^2/\mathrm{d}T^2)(F_S-F_N)$ from the corresponding free energy difference (F_S-F_N) which is calculated using a generalized Bardeen–Stephen formula[28]. The normal-state specific heat is calculated to be $C_N=\gamma_nT$ with $\gamma_n=2.62\,\mathrm{mJ\,mol^{-1}\,K^{-2}}$ (ref. 16). Symbols are the results of experimental measurements[3–5], and the dashed curve is the standard one-gap BCS prediction corresponding to a transition temperature of 39.4 K.

ious spectroscopic measurements[6–9], but a direct quantitative comparison requires knowledge of various physical parameters involved in a specific experiment.

A direct quantitative comparison between theory and measurement is possible, however, for the specific heat. The measured specific heat[3–5] of MgB_2 at low temperature is substantial, and a large hump appears at about 10 K that is inconsistent with a one-gap BCS model. We have calculated the specific heat from the free energy of the superconducting state. The overall shape and magnitude of our calculated specific-heat curve agrees very well with the experimental data, especially below 30 K (Fig. 4). We find that the low-temperature hump in our calculated curve and in the experimental data is caused by the existence of low-energy excitations across the small superconducting energy gap of the π-bonding states. □

Received 14 November 2001; accepted 31 May 2002; doi:10.1038/nature00898.

1. Nagamatsu, J., Nakagawa, N., Muranaka, T., Zenitani, Y. & Akimitsu, J. Superconductivity at 39 K in magnesium diboride. *Nature* **410,** 63–64 (2001).
2. Hinks, D. G., Claus, H. & Jorgensen, J. D. The complex nature of superconductivity in MgB_2 as revealed by the reduced total isotope effect. *Nature* **411,** 457–460 (2001).
3. Wang, Y., Plackowski, T. & Junod, A. Specific heat in the superconducting and normal state (2-300 K, 0-16 T), and magnetic susceptibility of the 38 K superconductor MgB_2. *Physica C* **355,** 179–193 (2001).
4. Bouquet, F., Fisher, R. A., Phillips, N. E., Hinks, D. G. & Jorgensen, J. D. Specific heat of $Mg^{11}B_2$: evidence for a second energy gap. *Phys. Rev. Lett.* **87,** 047001-1–047001-4 (2001).
5. Yang, H. D. *et al.* Order parameter of MgB_2: a fully gapped superconductor. *Phys. Rev. Lett.* **87,** 167003-1–167003-1 (2001).
6. Szabo, P. *et al.* Evidence for two superconducting energy gaps in MgB_2 by point-contact spectroscopy. *Phys. Rev. Lett.* **87,** 137005-1–137005-4 (2001).
7. Giubileo, F. *et al.* Two-gap state density in MgB_2: a true bulk property or a proximity effect? *Phys. Rev. Lett.* **87,** 177008-1–177008-4 (2001).
8. Chen, X. K., Konstantinovi, M. J., Irwin, J. C., Lawrie, D. D. & Franck, J. P. Evidence for two superconducting gaps in MgB_2. *Phys. Rev. Lett.* **87,** 157002-1–157002-4 (2001).
9. Tsuda, S. *et al.* Evidence for a multiple superconducting gap in MgB_2 from high-resolution photoemission spectroscopy. *Phys. Rev. Lett.* **87,** 177006-1–177006-4 (2001).
10. Kortus, J., Mazin, I. I., Belashchenko, K. D., Antropov, V. P. & Boyer, L. L. Superconductivity of metallic boron in MgB_2. *Phys. Rev. Lett.* **86,** 4656–4659 (2001).
11. An, J. M. & Pickett, W. E. Superconductivity of MgB_2: covalent bonds driven metallic. *Phys. Rev. Lett.* **86,** 4366–4369 (2001).
12. Bohnen, K.-P., Heid, R. & Renker, B. Phonon dispersion and electron-phonon coupling in MgB_2 and AlB_2. *Phys. Rev. Lett.* **86,** 5771–5774 (2001).
13. Yildirim, T. *et al.* Giant anharmonicity and nonlinear electron-phonon coupling in MgB_2: a combined first-principles calculation and neutron scattering study. *Phys. Rev. Lett.* **87,** 037001-1–037001-4 (2001).
14. Liu, A. Y., Mazin, I. I. & Kortus, J. Beyond Eliashberg superconductivity in MgB_2: anharmonicity, two-phonon scattering, and multiple gaps. *Phys. Rev. Lett.* **87,** 087005-1–087005-4 (2001).
15. Kong, Y., Dolgov, O. V., Jepsen, O. & Andersen, O. K. Electron-phonon interaction in the normal and superconducting states of MgB_2. *Phys. Rev. B* **64,** 020501-1–020501-4 (2001).
16. Choi, H. J., Roundy, D., Sun, H., Cohen, M. L. & Louie, S. G. First-principles calculation of the superconducting transition in MgB_2 within the anisotropic Eliashberg formalism. Preprint cond-mat/0111182 at ⟨http://xxx.lanl.gov⟩ (2001).
17. Eliashberg, G. M. Interactions between electrons and lattice vibrations in a superconductor. *Zh. Eksp. Teor. Fiz.* **38**, 966–976 (1960); *Sov. Phys. JETP* **11**, 696–702 (1960).
18. Allen, P. B. & Mitrović, B. in *Solid State Physics* (eds Ehrenreich, H., Seitz, F. & Turnbull, D.) Vol. 37 1–92 (Academic, New York, 1982).
19. Carbotte, J. P. Properties of boson-exchange superconductors. *Rev. Mod. Phys.* **62,** 1027–1157 (1990).
20. Marsiglio, F., Schossmann, M. & Carbotte, J. P. Iterative analytic continuation of the electron self-energy to the real axis. *Phys. Rev. B* **37,** 4965–4969 (1988).
21. Karapetrov, G., Iavarone, M., Kwok, W. K., Crabtree, G. W. & Hinks, D. G. Scanning tunneling spectroscopy in MgB_2. *Phys. Rev. Lett.* **86,** 4374–4377 (2001).
22. Sharoni, A., Felner, I. & Millo, O. Tunneling spectroscopy and magnetization measurements of the superconducting properties of MgB_2. *Phys. Rev. B* **63,** 220508-1–220508-4 (2001).
23. Rubio-Bollinger, G., Suderow, H. & Vieira, S. Tunneling spectroscopy in small grains of superconducting MgB_2. *Phys. Rev. Lett.* **86,** 5582–5584 (2001).
24. Schmidt, H., Zasadzinski, J. F., Gray, K. E. & Hinks, D. G. Energy gap from tunneling and metallic contacts onto MgB_2: possible evidence for a weakened surface layer. *Phys. Rev. B* **63,** 220504-1–220504- 4 (2001).
25. Takahashi, T., Sato, T., Souma, S., Muranaka, T. & Akimitsu, J. High-resolution photoemission study of MgB_2. *Phys. Rev. Lett.* **86,** 4915–4917 (2001).
26. Buzea, C. & Yamashita, T. Review of superconducting properties of MgB_2. *Supercond. Sci. Technol.* **14,** R115–R146 (2001).
27. Suhl, H., Matthias, B. T. & Walker, L. R. Bardeen-Cooper-Schrieffer theory of superconductivity in the case of overlapping bands. *Phys. Rev. Lett.* **3,** 552–554 (1959).
28. Bardeen, J. & Stephen, M. Free-energy difference between normal and superconducting states. *Phys. Rev. A* **136,** 1485–1487 (1964).

Acknowledgements

This work was supported by the National Science Foundation and by the Director, Office of Science, Office of Basic Energy Sciences of the US Department of Energy.

Computational resources have been provided by the National Science Foundation at the National Center for Supercomputing Applications and by the National Energy Research Scientific Computing Center. H. S. acknowledges financial support from the Berkeley Scholar Program funded by the Tang Family Foundation.

Competing interests statement

The authors declare that they have no competing financial interests.

Correspondence and requests for materials should be addressed to S.G.L. (e-mail: sglouie@uclink.berkeley.edu).

The influence of a chemical boundary layer on the fixity, spacing and lifetime of mantle plumes

A. Mark Jellinek & Michael Manga

Department of Earth and Planetary Science, University of California, Berkeley, California 94720, USA

Seismological observations provide evidence that the lowermost mantle contains superposed thermal and compositional boundary layers[1] that are laterally heterogeneous[2,3]. Whereas the thermal boundary layer forms as a consequence of the heat flux from the Earth's outer core, the origin of an (intrinsically dense) chemical boundary layer remains uncertain[4]. Observed zones of 'ultra-low' seismic velocity[5] suggest that this dense layer may contain metals[6,7] or partial melt[8], and thus it is reasonable to expect the dense layer to have a relatively low viscosity. Also, it is thought that instabilities in the thermal boundary layer could lead to the intermittent formation and rise of mantle plumes. Flow into ascending plumes can deform the dense layer, leading, in turn, to its gradual entrainment[9–14]. Here we use analogue experiments to show that the presence of a dense layer at the bottom of the mantle induces lateral variations in temperature and viscosity that, in turn, determine the location and dynamics of mantle plumes. A dense layer causes mantle plumes to become spatially fixed, and the entrainment of low-viscosity fluid enables plumes to persist within the Earth of hundreds for millions of years.

Convective motions driven by core cooling have a structure that is three-dimensional and time-dependent. Consequently, the dynamics of the interaction between this flow and an underlying dense layer is complex. Because of the computational challenge of resolving small (kilometre) length scales while tracking viscosity and density interfaces[15], numerical simulations for conditions appropriate to mantle convection are typically limited to two dimensions[12,13], though three-dimensional simulations are currently being performed[14]. Laboratory experiments are thus often used to study thermochemical convection, and the experiments presented here extend previous investigations[9,10,16] to the situation in which the dense layer is thin and has a low viscosity. Here we need to distinguish 'plumes' from 'thermals': we use 'plume' to describe buoyant upwellings (or downwellings) that extend continuously from the hot (or cold) boundary layer, and 'thermal' to indicate a discrete buoyant blob. Under conditions of thermal equilibrium, more-viscous cold fluid descends in narrow sheet-like plumes[17], whereas lower-viscosity hot fluid ascends mostly in thermals[18,19].

Our experiments are performed in the tank illustrated in Fig. 1 (the legend in Fig. 1 also defines the parameters and variables). An initial series of 23 experiments without a dense layer is performed to provide a framework to interpret the more complicated situation